Water Air Soil Pollut (2017) 228: 5
DOI 10.1007/s11270-016-3190-7

The Removal of Arsenic and Uranium from Aqueous Solutions by Sorption onto Iron Oxide-Coated Zeolite (IOCZ)

E. N. Bakatula · R. Molaudzi · P. Nekhunguni · H. Tutu

Received: 18 August 2016 / Accepted: 22 November 2016 / Published online: 5 December 2016
© Springer International Publishing Switzerland 2016

Abstract In this study, an iron oxide-coated zeolite (IOCZ) nanocomposite was synthesized and used for the removal of U(VI) and As(III) from aqueous solutions using a batch system. Parameters such as various contact times, pH, competing ions (Cd^{2+}, Co^{2+}, and Cr^{3+}), temperature, and initial concentrations of uranium(VI) and arsenic(III) were investigated. The experimental results were fitted to the Langmuir, Freundlich, and Dubinin–Radushkevich isotherms to obtain the characteristic parameters of each model. Results suggested that adsorption of U(VI) and As(III) by IOCZ was best modeled with the Freundlich isotherm. The kinetic experimental data fitted the pseudo second-order model better than the pseudo first-order model for both elements. Using the thermodynamic equilibrium constants obtained at different temperatures, various thermodynamic parameters, such as ΔG^{o}, ΔH^{o}, and ΔS^{o}, were calculated. These parameters indicated that the process is spontaneous and exothermic in nature. It was noted that an increase in temperature resulted in a decrease of 8.5 and 27.5% for U and As removal, respectively. An increase in initial concentrations of U(VI) and As(III) from 10 to 100 mg L^{-1} at pH 3 resulted in increased adsorption capacities (q_e) for both elements. The increases were from 1.247 to 20.10 mg g^{-1} for U(VI) and from 3.115 to 54.18 mg g^{-1} for As(V). The presence of competing ions such as Cd^{2+}, Co^{2+}, and Cr^{3+} enhanced the removal of As by 9.2% whereas the adsorption capacity of uranium decreased by 13.8%. This research demonstrated that IOCZ is a potential adsorbent for the removal of U(VI) and As(III) from aqueous solutions.

Keywords Iron oxide-coated zeolite · Arsenic · Uranium · Adsorption · Isotherms

E. N. Bakatula (✉) · R. Molaudzi · P. Nekhunguni · H. Tutu

Molecular Sciences Institute, School of Chemistry, University of the Witwatersrand, Private Bag X3, Wits 2050, South Africa
e-mail: enbakatula@gmail.com

E. N. Bakatula
Civil, Geological and Mining Engineering Department, École Polytechnique de Montréal, Montreal, QC H3C 3A7, Canada

1 Introduction

Aquatic systems are prone to contamination by toxic elements such as Cr, As, Pb, Hg, Cd, and U. Largely, these elements emanate from mining and smelting operations and can find their way into aquatic systems via dust fallout, erosion, and weathering of waste as well as leachate solutions emanating from such sources. In South Africa, for instance, U and As are commonly found in gold mining waste in the Witwatersrand Basin. The basin has contributed immensely to the development of the city of Johannesburg and the economy through vast amounts of gold that have been mined in it, accounting for over half of the gold ever mined in the world (Robb and Robb 1998). The waste from the mining activities is contained in tailing dumps that are scattered along the mining belt stretching in an east–west direction across the south of Johannesburg. Several studies in the basin have reported that the dust and

leachates emanating from the dumps contain significant amounts of contaminants, among them U and As (Winde 2002; Winde and Sandham 2004; Reimold and Gibson 2006; Tutu et al. 2008; Tutu et al. 2009; McCarthy and Pretorius 2009; Winde 2010; Bakatula 2012). U and As occur as uraninite (UO_2), brannerite (UTi_2O_6), arsenopyrite (FeAsS), cobaltite (CoAsS), and gersdofite (NiAsS) in the host ores (Feather and Koen 1975).

In oxidizing environments, uranium occurs as the uranyl ion, UO_2^{2+}, in which it has a valence of VI. Uranium is both chemotoxic and radioactive with the liver and kidneys being the main targets of uranium's toxic effects and with reservoirs of uranium concentrating in the kidneys and bones (WHO 2005; Hakonson-Hayes et al. 2002). This radionuclide makes its way into the human body through eating, drinking, and inhaling dust particles (DWAF 2015; Osborne and Ehrlich 1976). The allowed limit of uranium in drinking water according to South African guideline is 0.07 mg L^{-1} (DWAF 2015). The toxicity of arsenic depends on the specific chemical form. Inorganic trivalent arsenite (As^{III}) is 2–10 times more toxic than pentavalent arsenate (As^{V}) (Ferguson and Gavis 1972), whereas the toxicity of organo-arsenicals is generally lower than that of its inorganic species. Inorganic forms of arsenic most often exist in aqueous systems. Arsenic is sensitive to mobilization at pH between 6.5 and 8.5 and under both oxidizing and reducing conditions (Smedley and Kinniburgh 2003). Contamination with high levels of arsenic is of concern because it can cause a number of human health effects. Several epidemiological studies have reported a strong association between arsenic exposure and increased risks of both carcinogenic and systemic health effects (Tchounwou et al. 2003). Interest in the toxicity of arsenic has been heightened by recent reports of large populations in West Bengal, Bangladesh, Thailand, Inner Mongolia, Taiwan, China, Mexico, Argentina, Chile, Finland, and Hungary that have been exposed to high concentrations of arsenic in their drinking water and are displaying various clinico-pathological conditions including cardiovascular and peripheral vascular disease, developmental anomalies, neurologic and neurobehavioral disorders, diabetes, hearing loss, portal fibrosis, hematologic disorders (anemia, leukopenia, and eosinophilia), and carcinoma (Tchounwou et al. 2004; Agency for Toxic Substances and Disease 2000; Centeno et al. 2005; National Research Council 2001).

In South Africa, severe arsenic poisoning has been reported in the Northern Cape and Limpopo provinces where concentrations of 1000 μg/L were found in groundwater (Sami and Druzynski 2003). Another source of arsenic to groundwater and the soil in South Africa is the use of chromated copper–arsenate in the preservation of timber. Arsenic actually protects the timber from wood-destroying insects. Improper disposal of waste from timber plants contaminates the soil and water systems around the plants (Kesunathan et al. 2006). Significant amounts of arsenic have also been reported in mine leachates and tailings in the Witwatersrand Basin (Tutu 2006). The allowed limit of arsenic in drinking water according to South African guideline is 10 μg L^{-1} (DWAF 2015).

Iron oxides have proved to be an effective sorbent for the removal of various contaminants from water, due to their characteristics such as high surface area and surface charge, as well as high affinity towards metals and metalloids. When used by themselves, iron oxides are difficult to remove from water after adsorption and thus need to be placed as a coating onto particles to provide mechanical stability (Thirunavukkarasu et al. 2003; Hsu et al. 2008). Iron-based oxides have been found to adsorb arsenic compounds in drinking water to a significant extent. For instance, Yuan et al. (2002) evaluated several iron-treated natural materials, such as Fe-treated activated carbon (FeAC), Fe-treated gel beads (FeGB), and iron oxide-coated sand (IOCS), for removing arsenic in drinking water for household use (cooking and drinking) and showed that IOCS had a good performance in terms of As(III) and As(V) removal in batch tests, column tests, and field experiments. Yean et al. (2005) evaluated the sorption and desorption behavior of arsenic to magnetite (Fe_3O_4) nanoparticles, and they found that the sorption capacity was dependent on the pH value and surface area of the adsorbent.

Coating iron oxide onto particles with natural affinity for cations (such as zeolites) and high surface area may provide an effective sorption media with the application for both cationic and anionic contaminants from water.

The aim of this work was to assess the performance of iron oxide-coated zeolite (IOCZ) in removing U and As from aqueous solutions. The approach was based on conducting batch studies to assess the effect of pH, initial concentrations of U and As, contact time, temperature, and the presence of competing ions (Cd^{2+}, Co^{2+}, and Cr^{3+}). The insight on the processes gained in this study is useful for systems in which initially

zeolite is used as the adsorbent, but the precipitation of Fe out of the solutions being treated leads to the inadvertent coating of the zeolite.

2 Materials and Methods

2.1 Preparation of Iron Oxide-Coated Zeolite

Natural zeolite was provided by the School of Animal, Plant and Environmental Sciences, University of the Witwatersrand, South Africa. The natural zeolite was treated with NaOH to obtain the activated zeolite–sodium type used for the synthesis of the IOCZ. Na–zeolite was obtained by soaking 100 g of natural zeolite (fraction 2–3 mm) in 1000 mL of 2 mol L^{-1} NaOH for 24 h at room temperature (i.e., 25 ± 1 °C). The zeolitic material was repeatedly washed with deionized water to remove any excess Na and then dried at room temperature.

In the first step, iron oxide (magnetite) particles were prepared by adding a 2 mol L^{-1} NaOH solution drop by drop (with agitation) to a 1000 mL solution containing 4.5 g of ferrous sulfate until the pH reached 11. The resulting slurry (essentially iron hydroxide) was then heated in a water bath to form iron oxide which was then washed with deionized water and dried at room temperature.

In the second step, iron oxide particles (2.0 g) were re-dispersed in deionized water and Na–zeolite (6.0 g) was added slowly with agitation at a ratio of 3:1 (*w*/*w*) zeolite/iron oxide.

The IOCZ obtained was washed with deionized water, dried at room temperature, and crushed to particle size (<2 mm) using a mortar and pestle.

2.2 Physical–Chemical Characterization of the Natural Zeolite and IOCZ

Natural zeolite was characterized using X-ray fluorescence (chemical composition, performed in the School of Geosciences at University of the Witwatersrand, South Africa) and FTIR (Tensor 27, Bruker, Germany) (for the identification of functional groups). The surface area and cationic exchange capacity (CEC) were determined by the Brunauer–Emmet–Teller (BET surface area and porosity analyzer, (Tristar 3000 Analyzer, Micromeritics, USA) and $BaCl_2$ methods Gillman and Sumpter (1986), respectively. The zeolite–iron oxide particles were characterized using the Fourier transform infrared (FTIR) and X-ray diffraction (XRD).

The point of zero charge (PZC) for the IOCZ was determined using the salt addition method (Tan et al. 2008; Mahmood et al. 2011). In the method, a sample mass of 0.200 g was added to 40.0 mL of 0.1 mol L^{-1} $NaNO_3$ solution. The pH was adjusted using a pH Benchtop meter (Thermo Scientific Orion Star A211, Germany) to 2, 3, 4, 5, 6, 7, 8, 9, 10, and 11 (±0.1 pH units), with 0.1 mol L^{-1} HNO_3 and 0.1 mol L^{-1} NaOH as needed in each centrifuge tube. These were then shaken for 24 h in an automated shaker (Labcon, South Africa) at 150 rpm to reach equilibrium. After settling, the final pH of each suspension was measured carefully. The ΔpH (the difference between final and initial pH) values were then plotted against the initial pH values. PZC was the pH value where ΔpH equals zero. Each set of experiments was done in triplicate, and the mean value was recorded.

2.3 Preparation of Stock Solutions

All chemicals used were of analytical grade and were purchased from Merck, South Africa. Uranium(VI) and arsenic(III) stock solutions of 1000 mg L^{-1} were prepared by dissolving appropriate amounts of $UO_2(NO_3)_2{\cdot}6H_2O$ and $NaAsO_2$, respectively, in deionized water. Working solutions were prepared by serial dilution of the stock solutions. Three solutions of 10 mg L^{-1} of co-ions, including Cd^{2+}, Co^{2+}, and Cu^{2+}, respectively, were prepared by the dissolution of known mass of their nitrate salts with deionized water. The initial pH values of the working solutions were adjusted by the addition of 0.5 mol L^{-1} NaOH or HNO_3 solutions.

In order to minimize the contamination of the samples, all glassware and polypropylene vessels were cleaned by soaking in detergent solution then acid bath and in deionized water each for 24 h. Before use, the vessels were rinsed several times with deionized water and air-dried.

2.4 Batch Adsorption Experiments

The setup of the two separate batches of experiments was the same for uranium and arsenic. In each case, elemental concentration, pH, kinetic, temperature, and effect of competing ions were assessed. The different procedures are described in paragraphs below.

2.4.1 Elemental Concentration Study

The effect of elemental concentration was studied by adding 1.0 g of IOCZ into polypropylene bottles containing 50 mL of U or As solutions at concentrations of 10, 20, 50, and 100 mg L^{-1}. The pH level of the solutions was adjusted with 0.1 mol L^{-1} solution $NaOH/HNO_3$ to the given pH value of 3. The mixture was shaken using an automated shaker (Labcon, SA) at 150 rpm for 5 h at a constant temperature (25 ± 1 °C). The optimum contact time evaluated from the kinetic experiments was used to perform these studies. The supernatant was filtered through a 0.45-μm pore cellulose nitrate membrane and then analyzed using an inductively coupled plasma optical emission spectroscopy (ICP-OES) (Kleve, Germany).

2.4.2 pH Study

The effect of varying solutions of pH on adsorbent performance was conducted by adding 1.0 g of IOCZ into polypropylene bottles containing 50 mL of 20 mg L^{-1} U or As solutions. The pH was varied by adding diluted solution of NaOH or HNO_3 dropwise to achieve pH values of 3, 5, and 8. The mixtures were agitated using automated shaker (Labcon, SA) at 150 rpm for 5 h at a constant temperature (25 ± 1 °C). After equilibration, the mixture was filtered through a 0.45-μm pore cellulose nitrate membrane. The supernatant was analyzed using an ICP-OES (Kleve, Germany).

2.4.3 Kinetic Study

The kinetic experiments were performed in a 1-L beaker containing 500 mL of 20 mg L^{-1} U(V) or As(III) solutions and 10.0 g of IOCZ. Solutions of uranium and arsenic were adjusted at pH 3 using diluted HNO_3. The mixture was shaken in an automated shaker (Labcon, SA) at 78 rpm, and the temperature was kept constant at 25 ± 1 °C. Samples were withdrawn at pre-determined time intervals (20, 30, 60, 90, 120, 150, and 180 s). The volume withdrawn at each pre-determined time was 5 mL (i.e., 1% of the total volume) to minimize the change in the ratio of elemental concentration to the adsorbent mass. The supernatant was analyzed using ICP-OES (Kleve, Germany).

2.4.4 Temperature Study

The effect of temperature was studied by adding 1.0 g of IOCZ into polypropylene bottles containing 50 mL of 20 mg L^{-1} U or As solutions at pH 3. The mixture was shaken at 24 and 30 °C (i.e., 297.15 and 303.15 K, respectively) using an automated shaker (Labcon, SA) set at 150 rpm for 5 h. At equilibrium, the mixture was filtered and the filtrate was analyzed by ICP-OES (Kleve, Germany).

2.4.5 The Presence of Competing Ions

The study of the effect of the presence of competing ions was done by adding 1.0 g of IOCZ into polypropylene bottles containing 50 mL of a mixture of Cd^{2+}, Cr^{3+}, and Cu^{2+}. U and As solutions were added to each bottle such that their concentrations were 10 mg L^{-1} while that of competing ions was 5 mg L^{-1}. The obtained mixtures (multi-ion solution and IOCZ) were shaken using an automated shaker (Labcon, USA) for 5 h at 150 rpm, and the temperature was kept constant at 25 ± 1 °C. At equilibrium, the mixture was filtered and the filtrate was analyzed by ICP-OES (Kleve, Germany).

All analyses were based on triplicate measurements with analytical errors (relative standard deviation) less than 10%.

2.5 Modeling of Analytical Results

2.5.1 Adsorption Capacity

The adsorption capacity (q_e) of IOCZ was calculated under various conditions using the following expression (Eq. (1)):

$$q_e = \frac{(C_0 - C_e)V}{M} \quad (1)$$

where C_0 is the initial U or As concentration in milligrams per liter and C_e the U or As concentration at equilibrium in milligrams per liter, V the volume of U or As solution (L), and M the mass of IOCZ adsorbent (g).

2.5.2 Adsorption Isotherms

The equilibrium adsorption isotherm is of importance in the design of adsorption systems (Langmuir 1918; Freundlich 1906; Dada et al. 2012). The equilibrium data obtained in the present study were analyzed using

the linear forms of the expressions of the Langmuir (Eq. (2)), Freundlich (Eq. (3)), and Dubinin–Radushkevich (D-R) (Eqs. (4) and (5)) isotherm models:

$$\frac{C_e}{q_e} = \frac{1}{q_m \cdot b} + \frac{C_e}{q_m} \tag{2}$$

$$\log q_e = \log K_F + \frac{1}{n} \cdot \log C_e \tag{3}$$

$$\ln(qe) = \ln(Xm) + \beta * F^2 \tag{4}$$

$$F = R*T*\ln\left(1 + 1/Ce\right) \tag{5}$$

where forEqs. (2) and (3), C_e is the equilibrium concentration (mg L^{-1}), q_e is the amount adsorbed at equilibrium (mg g^{-1}), q_m is the maximum amount of adsorbate per unit weight of adsorbent to form a complete monolayer on the surface (mg g^{-1}), b is the Langmuir isotherm constant (L mg^{-1}), related to the affinity of the adsorption sites, and K_F ((mg g^{-1}) (L $mg^{-1})^{1/n}$) and n are the Freundlich constants related to adsorption capacity and adsorption intensity of adsorbents, respectively.

For Eq. (4), Xm is the maximum sorption capacity of sorbent (mol/kg), β is a constant related to mean sorption energy (mol^2/kJ^2), F is the Polanyi potential, R is the gas law constant (kJ/(mol K)), and T is the absolute temperature (K).

The constants β and Xm were obtained from the slope and intercept of the plot of ln(qe) vs. F^2. The sorption energy (E_s) (kJ mol^{-1}) is correlated with β (the isotherm constant) by the following relationship:

$$E_s = \frac{1}{\sqrt{-2 \cdot \beta}}. \tag{6}$$

If E_s is less than 8 kJ mol^{-1}, the adsorption process is physisorption (i.e., an ion–ion attraction); if E_s is between 8 and 16 kJ mol^{-1}, the adsorption process is by ion exchange; and if E_s is greater than 16 kJ mol^{-1}, the adsorption process is chemisorption (typically via the formation of strong covalent bonds).

2.5.3 Adsorption Kinetic Study

The study of adsorption kinetics provides information about the mechanism of adsorption, which is important for the efficiency of the process and the prediction of the rate at which contaminants are removed from aqueous solutions. Several kinetic models are available to examine the controlling mechanism of the adsorption process and to test the experimental data.

The rate constants of the adsorbate removal from the solution by IOCZ composites were determined using the Lagergren pseudo first-order equation (Eq. (7)) (Aksu 2002; Fungaro et al. 2012) and the pseudo second-order equation (Eq. (8)) (Ho et al. 1999):

$$\log(q_e - q_t) = \log(q_e) - \frac{k_1 \cdot t}{2.303} \tag{7}$$

$$\frac{t}{q_t} = \frac{1}{k_2 \cdot q_e^2} + \frac{1}{q_e} \cdot t \tag{8}$$

where q_e is the amount of ion adsorbed at equilibrium (mg g^{-1}), q_t is the amount of ion adsorbed at time t (mg g^{-1}), k_1 is the rate constant for the pseudo first-order model (min^{-1}), and k_2 is the rate constant for the pseudo second-order model (g mg^{-1} min^{-1}).

2.5.4 Thermodynamic Study

The thermodynamic parameters, namely the Gibbs free energy change, ΔG^o (kJ mol^{-1}), enthalpy change, ΔH^o (kJ mol^{-1}), and entropy change, ΔS^o (kJ (mol K)$^{-1}$), for the specific adsorption were calculated using Eqs. (9) and (10) (Unlu and Ersoz 2007; Wang and Chen 2006):

$$\Delta G^o = -R.T.\ ln\ K_C \tag{9}$$

$$\Delta G^o = \Delta H^o - T(\Delta S^o) \tag{10}$$

where R is the universal gas constant (8.314 J mol^{-1} K^{-1}), T is the absolute temperature in Kelvin, and K_C is the equilibrium constant (L g^{-1}). Enthalpy change, ΔH^o, and entropy change, ΔS^o, were determined from the slope and intercept of the plot according to Eq. (10).

2.5.5 Mathematical Modeling and Statistical Interpretation

The validity for each model is found by the use of a normalized standard deviation $\Delta q(\%)$ which can be calculated from the following Eq. (11):

$$\Delta q(\%) = 100\sqrt{\frac{\sum_{i=1}^{n}\left[\frac{q_{\exp} - q_{calc}}{q_{\exp}}\right]^2}{n-1}} \tag{11}$$

where $q_{\exp}$ is the experimental metal ion removal, q_{cal} is the calculated amount of metal ions adsorbed, and n is the number of data points.

The goodness-of-fit of the models to the experimental data is found by the comparison of the correlation coefficients (i.e., R^2).

2.5.6 Elemental Speciation Study

The speciation of U and As in solution was studied using the Hydra and MEDUSA geochemical modeling code database (Puigdomenech 1999). The code assumes a state of thermodynamic equilibrium for the solutions under consideration and based on this calculates the species distribution under the given solution conditions. It should be noted here that speciation models do not require any calibration as this is done intrinsically in the models.

3 Results and Discussion

3.1 Characterization of Zeolite

The chemical composition of the natural zeolite used in this study was performed using XRF and the results are presented in Table 1.

The cationic exchange capacity was 23.16 meq/100 g, obtained according to the $BaCl_2$ method with Na^+, K^+, Ca^{2+}, and Mg^{2+} being the exchangeable cations in the zeolite cavities (Gillman and Sumpter 1986). The surface area and the average pore volume were 18.07 m^2/g and 0.0968 cm^3/g, respectively.

FTIR and PXRD Analysis of Na–Zeolite and IOCZ Figure 1 shows the FTIR spectra for Na–zeolite (Na-Z) as well as that for the IOCZ. Peaks were depicted at 3434 cm^{-1} (O–H stretch); 1631 cm^{-1} (O–H bend); 1106 cm^{-1} (Si–O) and 795 cm^{-1} (Al–O); and 536 cm^{-1} (O–H bend out of plane). The presence of iron oxide was confirmed by the new peak at 2925 cm^{-1}.

Table 1 Chemical composition of the natural zeolite

Constituent	Value (%)
SiO_2	77.36
Al_2O_3	12.96
CaO	1.42
Fe_2O_3	0.13
Na_2O	1.62
K_2O	4.0
MgO	0.92
LOI	11.96

The powder X-ray diffraction (PXRD) patterns (not shown here) depicted clinoptilolite ($(Na,K,Ca)_{2-3}Al_3(Al,Si)_2\ Si_{13}\ O_{36}12H_2O$) as the predominant mineral in the natural zeolite. The PXRD pattern of IOCZ revealed the presence of 23.98% of Fe_2O_3; an increase of 22.85% compared to natural zeolite confirms the coating of iron oxide on the surface of zeolite.

3.2 Adsorption Studies

3.2.1 Effect of Initial Uranium and Arsenic Concentration

The results for the adsorption of U and As with respect to change in initial concentration are presented in Fig. 2. The results showed an increase of adsorption capacity with an increase in the initial concentration from 10 to 100 mg L^{-1} for both elements. The results indicated that the adsorption capacity of U(VI) and of As(III) increased from 1.247 to 20.10 mg g^{-1} and from 3.115 to 54.18 mg g^{-1}, respectively, as the elemental concentration increased from 10 to 100 mg L^{-1}. The adsorption of As was generally higher (~2 times more) than that of uranium. The saturation point was not reached up to a concentration of 100 mg L^{-1} for both arsenic and uranium.

The increase may be attributed to more elemental ions being available for the adsorption sites as the concentrations increased. The higher adsorption of As compared to U will be explained later when the mechanisms of adsorption are assessed.

3.2.2 Adsorption Isotherms

As aforementioned, Langmuir, Freundlich, and Dubinin–Radushkevich (D-R) isotherms were used to quantitatively describe elemental sorption by IOCZ. The correlation coefficient (R^2) values were used to determine the most fitted model among all the three written above. The isotherm parameters as well as the related correlation coefficients are listed in Table 2.

Based on the correlation coefficient (R^2), the Freundlich model yielded a better fit for both elements ($R^2 = 0.942$ for U and 0.981 for As). The fit to the Freundlich isotherm may be attributed to the heterogenous distribution of active sites on the IOCZ surface (Bakatula et al. 2014). This model assumes adsorption onto a heterogenous surface where different sites could have different energies. The values of the mean free energy (*Es*) calculated from the D-R isotherm were

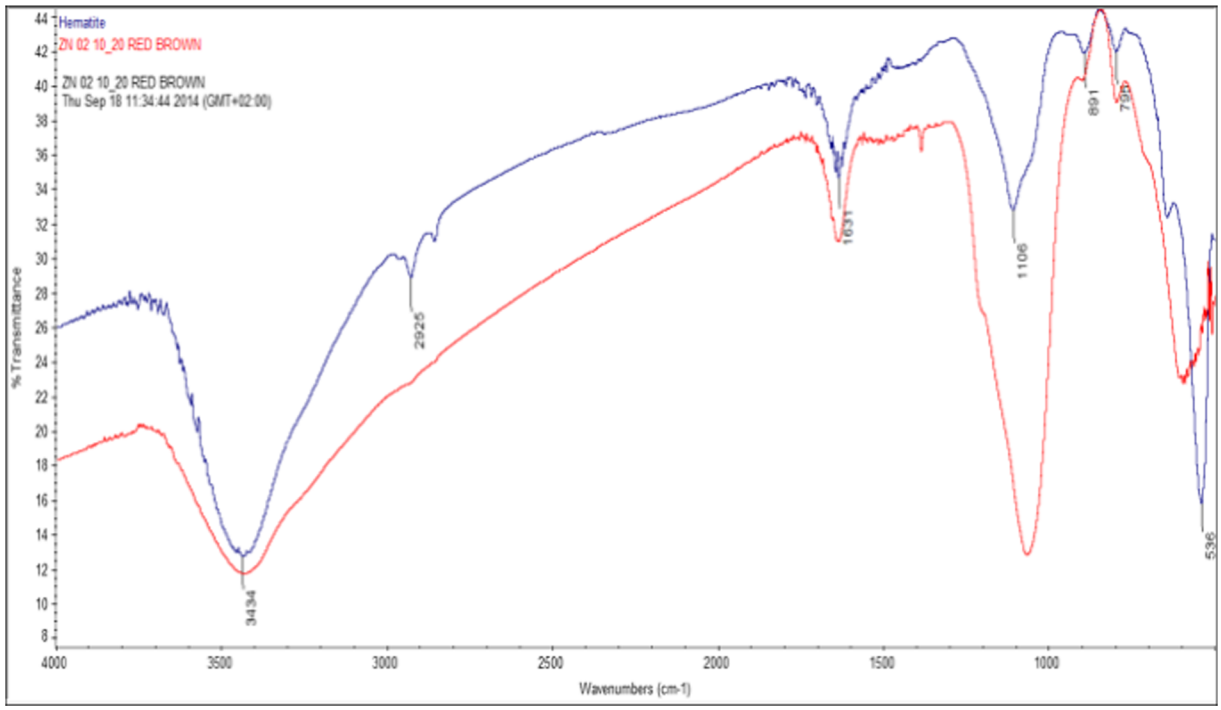

Fig. 1 FTIR spectra of Na–zeolite and IOCZ

8.213 kJ mol^{-1} for uranium and 8.895 kJ mol^{-1} for arsenic, indicating an ion exchange mechanism for both elements. The following mechanism is suggested:

Firstly, the charge on the surface of iron oxides results from the dissociation of the surface hydroxyl groups (Eq. (12)) (Wang et al. 2010).

$$Fe_2O_3 \xrightarrow[H_2O]{\text{Hydroxylation}} \equiv FeOH \begin{cases} \xrightarrow{\text{Protonation}} FeOH_2^+ \\ \xrightarrow{\text{Deprotonation}} FeO^- + H^+ \end{cases}$$

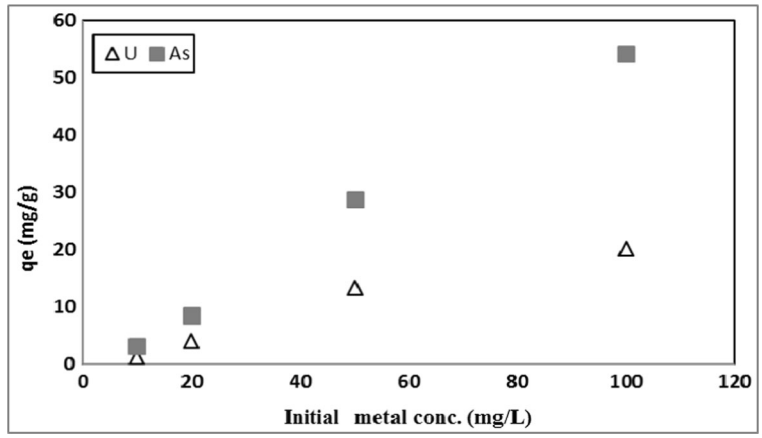

Fig. 2 Effect of U(V) and As(III) concentrations on their adsorption onto IOCZ (pH = 3, temp = 25 °C, contact time = 5 h) ($n = 3$ and RSD <10%)

Table 2 Langmuir, Freundlich, and D-R constant values for the sorption of U and As on IOCZ

	Langmuir constant				Freundlich constant				D-R constant			
	b (L mg^{-1})	q_m (mol kg^{-1})	R^2	Δq (%)	n	K_F (mg g^{-1})	R^2	Δq (%)	Xm (mol kg^{-1})	E_s (kJ mol^{-1})	R^2	Δq (%)
U	21,606	0.019	0.293	26.51	1.999	1.022	0.942	20.77	0.958	8.213	0.928	25.71
As	3889	0.034	0.623	21.24	1.893	1.012	0.981	11.28	0.919	7.295	0.947	36.73

Furthermore, the surface charge of iron oxide coated onto zeolite becomes more positive in acidic conditions due to protonation, resulting in an increase of adsorption sites for As (Jeon et al. 2009).

Secondly, the hydroxyl ion is exchanged with the arsenite ion:

$$\mathrm{Fe{-}OH} + \mathrm{H_2AsO_3^-} \rightarrow \mathrm{Fe{-}OAsO_2H} + \mathrm{OH^-}. \quad (13)$$

Previous studies revealed that sorption of As(V) as well as As(III) onto soil constituents, such as aluminum and iron oxides, happens through an inner-sphere complex via a ligand-exchange mechanism (Lumsdon et al. 1984; Sun and Doner 1996; Waychunas et al. 1993). This means that arsenic ions interacted with iron-modified zeolite surfaces in acid/base equilibrium, where underlying Fe ions act as a Lewis acid by exchanging the hydroxyl ion for other ligands to form surface complexes. Interaction between the surface hydroxyl groups and protons as well as ligand exchange provides iron oxides with high affinity to both arsenate and arsenite, both of which are Lewis bases (electron pair donors).

The maximum capacities q_m (mol kg^{-1}) determined from the Langmuir isotherm, defining the total capacity of IOCZ for uranium(VI) as well as As(III), were 0.019 and 0.034, respectively.

The Freundlich constant, K_F, (adsorption capacity, mg g^{-1}) values were 1.022 and 1.012, respectively, for uranium and arsenic. The subunitary values of the ratio $1/n$ suggest that the adsorption was favorable (Taffarel and Rubio 2010) and that the elements were bound with weak sorption energies (Özer et al. 1997). These results indicate that IOCZ has a very strong adsorption capacity for U(VI) and As(III) in the solution. When comparing the statistical results of the three models applied in this work (Table 2), the Freundlich isotherm was found to better predict the adsorption of U(VI) and As(III) onto IOCZ.

In previous studies, the Freundlich isotherm was reported to be suitable to represent arsenic adsorption processes by a wide range of iron containing adsorbents, including iron-pretreated activated carbon (Mondal et al. 2009), granular ferric hydroxide (Badruzzaman et al. 2004), and iron oxide-coated sand (Thirunavukkarasu et al. 2002).

3.2.3 The Effect of Initial pH

The initial pH of the solution is an important factor that must be considered during adsorption studies. The pH has two kinds of influence on elemental sorption, namely an effect on the solubility and speciation of the ions in

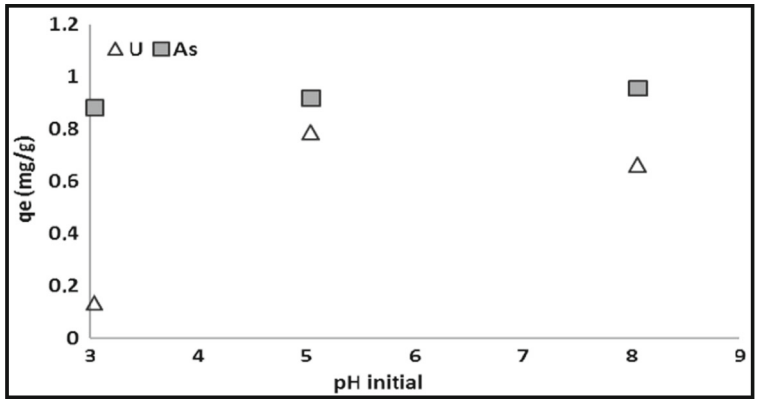

Fig. 3 Effect of pH on the adsorption of U and As on IOCZ (temp = 25 °C, C_i = 20 mg L^{-1}, contact time = 5 h) (n = 3 and RSD <10%)

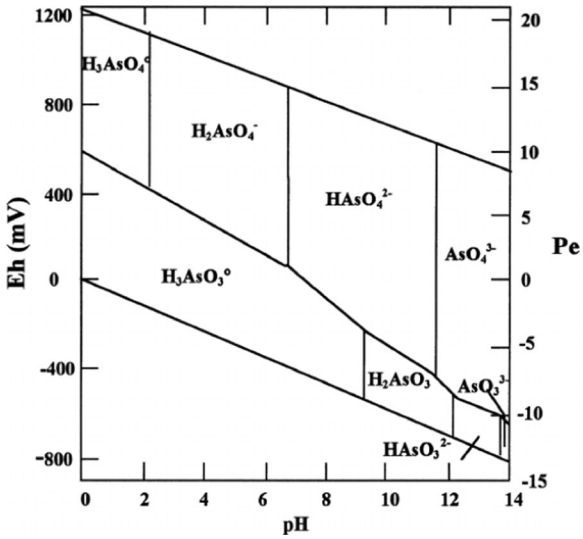

Fig. 4 Eh–pH diagram for aqueous arsenic species in the system AsO_2–H_2O at 25 °C (re-printed with permission from Smedley and Kinniburgh 2002)

solution and on the overall charge of the adsorbent. The adsorption of U and As was studied at pH 3, 5, and 8, which is the pH regime of most of gold mine waters in the Witwatersrand. The results of the effect of pH are shown in Fig. 3.

As seen in Fig. 3, the adsorption efficiency of As(III) on IOCZ was not much affected by the solution pH (pH 3 to 8). In fact, arsenic exists as oxyanions across pH ranges 2 to 8, as represented by the speciation diagram in Fig. 4. The diagram depicted $H_2AsO_4^-$ as the only dissolved species from pH 3 to 7 and $H_2AsO_4^{-2}$ at pH >7. Therefore, $(H_2AsO_4)^-$ being the most abundant species of As at the pH range studied, this explained the trend seen in the Fig. 3, almost no variation in adsorption capacity with the variation of solution pH. Similar trend was observed by Jeon et al. (2009) when adsorbing arsenic on iron-coated zeolite. As explained in the previous paragraph, the adsorption of arsenic on IOCZ followed an ion exchange process. This means that the surface charge of the adsorbent had no effect on the adsorption. Thus, it was concluded that adsorption of arsenic from aqueous solutions is independent of pH.

The relative abundance of various uranium(VI) species is a strong function of pH and composition of solution. The strong dependence of adsorption on pH can be explained by changes in the IOCZ surface charge and U speciation with pH. The pH_{PZC} of 10.4 means that at the pH range of the experiments, the surface charge of the IOCZ was positive. Thus, the predominance of U species will greatly influence its adsorption. The distribution of uranium species as a function of pH is presented in Fig. 5. At low pH (3–5), the UO_2^{2+} was predominant. Since both the uranyl ion and the adsorbent have net positive charges, the repulsion by the positive surface could explain the low removal of uranium by IOCZ. At pH 5–6, the neutral $UO_2(OH)_2{\cdot}H_2O$ (schoepite) was the most abundant species. This would likely precipitate on the adsorbent, and thus, the observed increase in adsorption may be a combination of precipitation and adsorption. At pH >6, negatively charged species, i.e., $UO_2(OH)_3^-$ and $UO_2(OH)_3^{2-}$, were dominant. More U would have been expected to be adsorbed, but the contrary was observed. This could suggest that the positively charged sites begin to

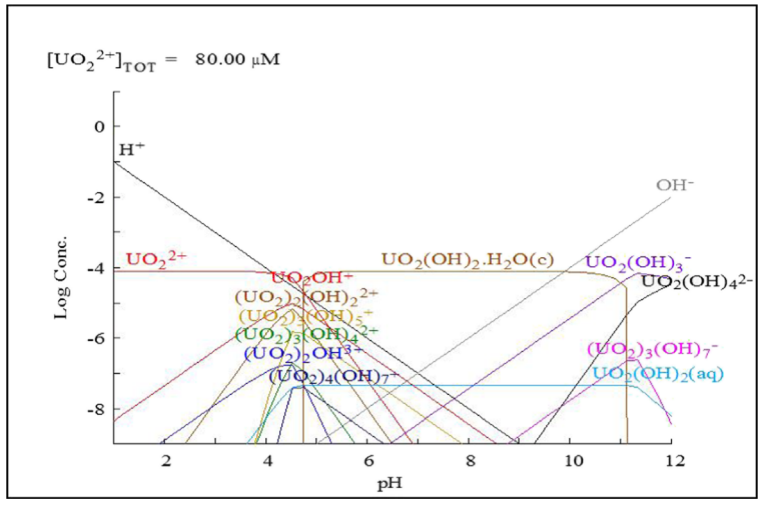

Fig. 5 Speciation of uranium in a uranium–water system at 25 °C and $I = 0$ M calculated using Hydra and MEDUSA speciation modeling freeware versions (Bakatula et al. 2015)

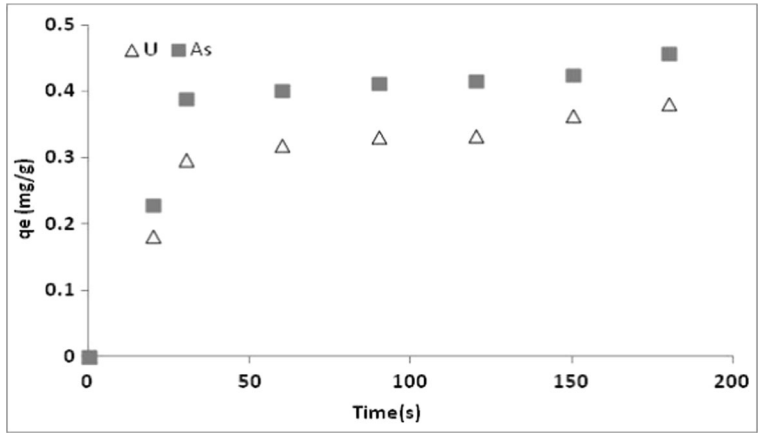

Fig. 6 Adsorption kinetics of U(VI) and As(III) onto IOCZ (temp = 25 °C, C_i = 20 mg L^{-1}, pH = 3) (n = 3 and RSD <10%)

decrease at those higher pH values that are close to the pH_{PZC}, leading to decreased adsorption of negatively charged U species.

Further work involving surface complexation modeling would have to be conducted to comprehensively understand the mechanism behind U adsorption as pH changes.

3.2.4 Adsorption Kinetics

Figure 6 illustrates adsorption kinetics of uranium and arsenic onto IOCZ. Adsorption kinetic studies showed a rapid removal of U(VI) and As(III) within the first 30 s to achieve equilibrium. The adsorption kinetics can be divided into two linear stages: (i) the rapid adsorption phase and (ii) the second stage of steady state, where the adsorption reached a plateau.

The change in the adsorption rate during adsorption could be explained by the availability of a large number of free adsorption sites on the surface of the adsorbent in the beginning of the reaction.

Kinetic Parameters The pseudo first-order and pseudo second-order models were applied to the kinetic data of uranium and arsenic adsorption onto IOCZ to investigate the mechanism of the adsorption process and determine the rate controlling step in the overall adsorption process. The kinetic parameters and correlation coefficients (R^2) for the two kinetic models were calculated from the linear plots of $\log(q_e - q_t)$ vs. t and t/q_t vs. t, respectively, and are listed in Table 3.

Based on the correlation coefficients, the pseudo second-order kinetic model represented the uranium and arsenic uptake best. The plots of q_t/t vs. t showed good linearity (Fig. 7) with high correlation coefficients (0.989 for U(VI) 0.991 and for As(III)). In addition, the equilibrium uptake calculated from the kinetic plots ($q_{e,cal}$) agreed well with the experimental values ($q_{e,exp}$, 0.363 and 0.421 mg/g for U(VI) and As(III), respectively.

Therefore, the sorption kinetics was well described by the pseudo second-order kinetics, which implied that the uranium and arsenic uptake by IOCZ was due to chemisorption.

The pseudo second-order kinetic model has been used to describe uranium and arsenic uptake by other iron containing adsorbents (Gu and Deng 2007; Guo and Chen 2005; Fierro et al. 2009).

Table 3 Kinetic parameters of the adsorption of U and As on IOCZ

Metal	Pseudo first-order				Pseudo second-order			
	k_1 min^{-1}	$q_{e(calc)}$ mg g^{-1}	R^2	Δq [%]	k_2 [mol (kg min)$^{-1}$]	$q_{e(calc)}$ mg g^{-1}	R^2	Δq [%]
U	0.151	1.208	0.864	88.35	49.48	0.348	0.989	13.14
As	0.129	1.149	0.736	86.23	17.06	0.459	0.995	14.67

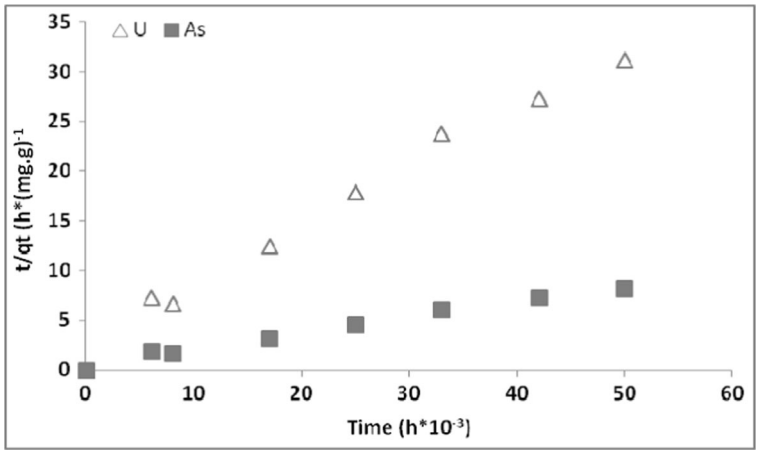

Fig. 7 Pseudo second-order kinetic model for the adsorption of uranium and arsenic on IOCZ

3.2.5 Effect of Temperature

The adsorption of U(VI) and As(V) was assessed at two different temperatures: 297.15 and 303.15 K. Thermodynamic parameters, i.e., enthalpy change (ΔH^o), free energy change (ΔG^o), and entropy change (ΔS^o), were calculated from the experimental data and the results are presented in Table 4. Raising the temperature of the metal solutions led to a decrease of the adsorption capacity of 8.5 and 27.5% for U and As, respectively. These results were confirmed by the negative values of enthalpy change, suggesting that the adsorption of both elements was exothermic. The $\Delta H°$ for the present process was found to be negative (−124.9 and −16.25 kJ mol^{-1}, for U and As, respectively), which proves the exothermic nature of the sorption reaction. The standard free energies ΔG^o for the sorption of uranium, obtained from Eq. (8), were −4.429 and 1.787 kJ mol^{-1} at 297.15 and 303.15 K, respectively. The negative value of ΔG^o depicts a spontaneous adsorption process. The standard free energy ΔG^o for As was close to 0 (0.138 kJ mol^{-1}), implying that the removal of As was spontaneous. A more positive ΔG^o with the increment of temperature implies a non-favorable reaction at higher temperature, which is a characteristic of exothermic surface process. The entropy changes (ΔS^o) were positive for both U and As, suggesting a high affinity of the elements for the IOCZ. This also confirms the increased randomness at the solid–solution interface during adsorption.

3.2.6 Effect of Competing Ions

The presence of competing ions, such as Cd^{2+}, Cr^{3+}, and Cu^{2+}, can have a significant effect on uranium and arsenic adsorption onto IOCZ. The results of the effect of competing ion studies are presented in Table 5. The presence of Cd^{2+}, Cr^{3+}, and Cu^{2+} decreased the percentage of U(VI) adsorption by 13.77%, whereas adsorption of As(III) increased slightly by 9.21%.

The concentrations of competing ions in this study are those likely to be encountered in wastewater from some mining areas in South Africa (Bakatula et al. 2015). Thus, IOCZ is able to remove uranium and arsenic even at the presence of competing ions investigated in this study.

Table 4 Thermodynamic parameters of U and As on IOCZ

Metal	*qe*		*Ea*	ΔH	ΔS	ΔG	
	mg g^{-1}		kJ mol^{-1}	kJ mol^{-1}	kJ (mol K)$^{-1}$	kJ mol^{-1}	
	297.15 K	303.15 K				297.15 K	303.15 K
U	0.992	0.907	129.8	−124.9	0.376	−4.429	1.787
As	0.946	0.686	107.2	−16.25	4.812	0.138	0.933

Table 5 Effect of the presence of competing ions (Cd^{2+}, Cr^{3+}, and Cu^{2+})

	Multi-ions solution q_e (mg g^{-1})	Single-ion solution q_e (mg g^{-1})
U	0.457	0.530
As	0.498	0.456
Cd	0.249	
Cu	0.248	
Cr	0.250	

4 Conclusion

In this study, iron oxide-coated zeolite (IOCZ) was synthesized and used for the removal of U(VI) and As(V) from aqueous solutions. The equilibrium of adsorption was suitably described by the Freundlich models, depicting that adsorption on a heterogeneous surface. The process of adsorption was relatively rapid and was best described by the pseudo second-order kinetic model. The thermodynamic models showed that the adsorption of U and As was spontaneous and followed exothermic processes. Furthermore, IOCZ was able to adsorb uranium and arsenic in the presence of competing ions such as Cd^{2+}, Cr^{3+}, and Co^{2+}.

Further work should focus on comprehensively understanding the adsorption at various pH values as surface complexation may be an important process. The findings of the study can be used to design and understand systems applying zeolite for contaminant removal from industrial and mine-polluted water.

Acknowledgements The authors express their sincere gratitude to the University Research Committee (URC) Postdoc Fellowship and the National Research Foundation for financial support.

References

Agency for Toxic Substances and Disease Registry (ATSDR). (2000). *Toxicological profile for arsenic TP-92/09*. Georgia: Center for Disease Control, Atlanta.

Aksu, Z. (2002). Determination of the equilibrium, kinetic and thermodynamic parameters of the batch biosorption of lead(II) ions onto Chlorella vulgaris. *Process Biochemistry, 38*, 89–99.

Badruzzaman, M., Westerhoff, P., & Knappe, D. (2004). Intraparticle diffusion and adsorption of arsenate onto granular ferric hydroxide (GFH). *Water Research, 38*(18), 4002–4012.

Bakatula, E.N. (2012). *Development of a biophysical system based on bentonite, zeolite and micro-organisms for remediating gold mine wastewaters and tailings ponds*. Thesis, University of the Witwatersrand, 7–12.

Bakatula, E. N., Cukrowska, E. M., Weiersbye, I. M., Mihaly-Cozmuta, L., Peter, A., & Tutu, H. (2014). Biosorption of trace elements from aqueous systems in gold mining sites by the filamentous green algae (*Oedogonium* sp.). *Journal of Geochemical Exploration*. doi:10.1016/j.gexplo.2014.02.017.

Bakatula, E. N., Mosai, A. K., & Tutu, H. (2015). Removal of uranium from aqueous solutions using ammonium-modified zeolite. *South African Journal of Chemistry, 68*, 165–171.

Centeno, J.A., Tchounwou, P.B., Patlolla, A.K, Mullick, F.G., Murakat, L., & al. (2005). Environmental pathology and health effects of arsenic poisoning: a critical review. In: Naidu R, Smith E, Smith J, Bhattacharya P, (eds.) *Managing arsenic in the environment: from soil to human health*. Adelaide.

Dada, A. O., Olalekan, A. P., & Olatunya, A. M. (2012). Langmuir, Freundlich, Temkin and Dubinin–Radushkevich isotherms studies of equilibrium sorption of Zn^{2+} unto phosphoric acid modified rice husk. *Journal of Applied Chemistry, 3*(1), 38–45.

Department of water affairs and forestry (DWAF). https://www.dwaf.gov.za/iwqs/wq_guide/domestic.pdf Accessed on 19 May, 2015.

Feather, C. E., & Koen, G. M. (1975). The mineralogy of the Witwatersrand reefs. *Minerals Science and Engineering, 7*, 189–224.

Ferguson, J. F., & Gavis, J. (1972). A review of the arsenic cycle in natural waters. *Water Research, 6*, 1259–1274.

Fierro, V., Muiz, G., Gonzalez-Sánchez, G., Ballinas, M., & Celzard, A. (2009). Arsenic removal by iron-doped activated carbons prepared by ferric chloride forced hydrolysis. *Journal of Hazardous Materials, 168*(1), 430–437.

Freundlich, H. M. F. (1906). Over the adsorption in solution. *The Journal of Physical Chemistry, 57*, 385–470.

Fungaro, D. A., Yamaura, M., & Craesmeyer, G. R. (2012). Uranium removal from aqueous solution by zeolite from fly ash-iron oxide magnetic nanocomposite. *International Review of Chemical Engineering, 4*(3), 353–358.

Gillman, G. P., & Sumpter, E. A. (1986). Modification to the compulsive exchange method for measuring exchange characteristics of soils. *Australian Journal of Soil Research, 24*, 61–66.

Gu, Z., & Deng, B. (2007). Use of iron-containing mesoporous carbon (IMC) for arsenic removal from drinking water. *Environmental Engineering Science, 24*(1), 113–121.

Guo, X., & Chen, F. (2005). Preparation and evaluation of GAC-based iron-containing adsorbents for arsenic removal. *Environmental Science and Technology, 39*, 6808.

Hakonson-Hayes, A. C., Fresquez, P. R., & Whicker, F. W. (2002). Assessing potential risks from exposure to natural uranium in well water. *Journal of Environmental Radioactivity, 59*, 29–40.

Ho, Y. S., Wase, D. A. J., & Forester, C. F. (1999). Kinetic studies of competitive heavy metal adsorption by sphagnum peat. *Environmental Technology, 17*, 441–443.

Hsu, J. C., Lin, C. J., Liao, C. H., & Chen, S. T. (2008). Removal of As(V) and As(III) by reclaimed iron-oxide coated sands. *Journal of Hazardous Materials, 153*, 817–826.

Jeon, C. S., Baek, K., Park, J. K., Oh, Y. K., & Lee, S. D. (2009). Adsorption characteristics of As(V) on iron-coated zeolite. *Journal of Hazardous Materials, 163*, 804–808.

Kesunathan, G., M. Tumelo, M., & Moodley, K.G. (2006). *Paper for the COST Action 37 Workshop,* Berlin.

Langmuir, I. (1918). The adsorption of gases on plane surfaces of glass, mica and platinum. *Journal of the American Chemical Society, 40*, 1361–1403.

Lumsdon, D. G., Fraser, A. R., Russell, J. D., & Livesey, N. T. (1984). New infrared band assignments for the arsenate ion adsorbed on synthetic goethite (a-FeOOH*). Journal of Soil Science, 35*, 381–386.

Mahmood, T., Saddique, M. T., Naeem, A., Westerhoff, P., Mustafa, S., et al. (2011). Comparison of different methods for the point of zero charge determination of NiO. *Industrial & Engineering Chemistry Research, 50*, 10017–10023.

McCarthy, T.S., & and Pretorius, K. (2009). Coal mining on the Highveld and its future water quality in the Vaal river system. *International Mine Water Association*, ISBN Number: 978-0-9802623-5-3.

Mondal, P., Mohanty, B., Majumder, C., & Bhandari, N. (2009). Removal of arsenic from simulated groundwater by GAC-Fe: a modeling approach. *AICHE Journal, 55*(7), 1860–1871.

National Research Council. Arsenic in drinking water. (2001) Update. On line http://www.nap.edu/books/0309076293/html/.

Osborne, S. H., & Ehrlich, H. L. (1976). Oxidation of arsenite by a soil isolate of Alcaligenes. *Journal of Applied Bacteriology, 41*, 295–305.

Özer, A., Ekiz, I. H., Özer, D., Kutsul, T., & Caglar, A. (1997). A comparative study of the biosorption of cadmium(II) ions to S. leibleinil and R. arrhizis. *Chimica Acta Turica, 25*(1), 63–67.

Puigdomenech, I. (1999). *MEDUSA: make equilibrium diagrams using sophisticated algorithms, version 2. Inorganic Chemistry*. Stockholm7 Royal Institute of Technology (KTH). http://www.inorg.kth.se.

Reimold, W. U., & Gibson, R.J. (2006). *Processes on the early earth, geological society of America*, pp 354.

Robb, L. J., & Robb, V. M. (1998). Gold in the Witwatersrand basin. In M. G. C. Wilson & C. R. Maske (Eds.), *The mineral resources of South Africa* (6th ed., pp. 294–349). Pretoria: Council of Geoscience.

Sami, K. & Druzynski, A.L. (2003). *Final report to the water research commission for the project* "*mapping of naturally occurring hazardous trace constituents in groundwater*". WRC Report No. 1236/1/03, South Africa.

Smedley, P. L., & Kinniburgh, D. G. (2002). A review of the source, behaviour and distribution of arsenic in natural waters. *Applied Geochemistry, 17*(5), 517–568.

Smedley, P.L. & Kinniburgh, D.G. (2003). *Source and behaviour of arsenic in natural waters, chapter 1, Arsenic report*, WHO, pp 60, British Geological Survey, Wallingford, Oxon OX10 8BB, U.K.

Sun, X., & Doner, H. E. (1996). An investigation of arsenate and arsenite bonding structures on goethite by FTIR. *Soil Science, 161*, 865–872.

Taffarel, R. S., & Rubio, J. (2010). Removal of Mn^{2+} from aqueous solution by manganese oxide coated zeolite. *Minerals Engineering, 23*, 1131–1138.

Tan, W. F., Lu, S. J., Liu, F., Feng, X. H., He, J. Z., & Koopal, L. K. (2008). Determination of the point of zero charge of manganese oxides with different methods including an improved salt titration method. *Soil Science, 173*, 277.

Tchounwou, P. B., Patlolla, A. K., & Centeno, J. A. (2003). Carcinogenic and systemic health effects associated with arsenic exposure—a critical review. *Journal of Toxicologic Pathology, 31*, 575–588.

Tchounwou, P. B., Centeno, J. A., & Patlolla, A. K. (2004). Arsenic toxicity, mutagenesis and carcinogenesis—a health risk assessment and management approach. *Molecular and Cellular Biochemistry, 255*, 47–55.

Thirunavukkarasu, O., Viraraghavan, T., Subramanian, K., & Tanjore, S. (2002). Organic arsenic removal from drinking water. *Urban Water, 4*(4), 415–421.

Thirunavukkarasu, O. S., Viraraghavant, T., & Subramanian, K. S. (2003). Arsenic removal from drinking water using iron oxide-coated sand. *Water, Air, and Soil Pollution, 142*, 95–111.

Tutu, H. (2006). *Determination and geochemical modeling of the dispersal of uranium in gold-mine polluted land on the Witwatersrand*. PhD Thesis, University Witwatersrand, Johannesburg.

Tutu, H., McCarthy, T. S., & Cukrowska, E. M. (2008). The chemical characteristics of acid mine drainage with particular reference to sources, distribution and remediation: the Witwatersrand Basin, South Africa, as a case study. *Applied Geochemistry, 23*, 3666–3684.

Tutu, H., McCarthy, T. S., Cukrowska, E. M., Hart, R., & Chimuka, L. (2009). Radioactive disequilibrium and geochemical modelling as evidence of uranium leaching from gold tailings dumps in the Witwatersrand Basin. *International Journal of Environmental Analytical Chemistry, 89*(8–12), 687–703.

Unlu, N., & Ersoz, M. (2007). Removal of heavy metal ions by using dithiocarbamated-sporopollenin. *Separation and Purification Technology, 52*, 461.

Wang, J., & Chen, C. (2006). Biosorption of heavy metals by Saccharomyces cerevisiae: a review. *Biotechnology Advances, 24*(5), 427–451.

Wang, J., Li, X., Scott, J. I., Yue, Z., & Economy, J. (2010). Iron oxide-coated on glass fibers for arsenic removal. *Separation Science and Technology, 45*(8), 1058–1065.

Waychunas, G. A., Rea, B. A., Fuller, C. C., & Davis, J. A. (1993). Surface chemistry of ferrihydrite. 1. EXAFS studies of the geometry of coprecipitated and adsorbed arsenate. *Geochimica et Cosmochimica Acta, 57*(15), 2251–2269.

Winde, F. (2002). Uranium contamination in fluvial systems—mechanisms and processes. Part I: geochemical mobility of uranium along the water path—the Koekemoerspruit (South Africa) as a case study. *Cuardernos de Investigacion Geografica, 28*, 49–57. ISSN 0211–6820.

Winde, F. (2010). U pollution in the Wonderfonteinspruit: 1997–2008 part I: U-toxicity, regional background and mining-related sources of U-pollution. *Water SA, 36*(3), 239–256.

Winde, F. & Sandham, L.A. (2004). Uranium pollution of South African streams—an overview of the situation in gold mining areas of the Witwatersrand. Sustainable Water Management

in Africa-Chances and Barriers. Supplement volume, *GeoJournal*, *61*, 131–149.

World Health Organization (WHO) (2005). Uranium in drinking water: background document for development of WHO guidelines for drinking water quality (WHO/SDE/WSH/03.04/118). *World Health Organization*, 26 pp.

Yean, S., Cong, L., Yavuz, C. T., Mayo, J. T., Yu, W. W., et al. (2005). Effect of magnetite particle size on adsorption and desorption of arsenite and arsenate. *Journal of Materials Research, 20*(12), 3255–3264.

Yuan, T., Hu, J. Y., Ong, S. L., Luo, Q. F., & Ng, W. J. (2002). Arsenic removal from household drinking water by adsorption. *Journal of Environmental Science and Health, Part A: Toxic/Hazardous Substances & Environmental Engineering, 37*(9), 1721–1736.